Fluid Flow through Porous Media: The Role of Stagnant Zones

J. S. Andrade, Jr.,[1] M. P. Almeida,[1] J. Mendes Filho,[1] S. Havlin,[2,3] B. Suki,[4] and H. E. Stanley[2]

[1]*Departamento de Física, Universidade Federal do Ceará, 60451-970 Fortaleza, Ceará, Brazil*
[2]*Center for Polymer Studies and Department of Physics, Boston University, Boston, Massachusetts 02215*
[3]*Minerva Center and Department of Physics, Bar-Ilan University, Ramat Gan, Israel*
[4]*Department of Biomedical Engineering, Boston University, Boston, Massachusetts 02215*

We investigate fluid flow through disordered porous media by direct simulation of the Navier-Stokes equations in a two-dimensional percolation structure. We find, in contrast to the log-normal distribution for the local currents found in the analog random resistor network, that over roughly 5 orders of magnitude the distribution $n(E)$ of local kinetic energy E follows a power law, with $n(E) \propto E^{-\alpha}$, where $\alpha = 0.90 \pm 0.03$ for the entire cluster, while $\alpha = 0.64 \pm 0.05$ for fluid flow in the backbone only. Thus the "stagnant" zones play a significant role in transport through porous media, in contrast to the dangling ends for the analogous electrical problem.   [S0031-9007(97)04671-1]

PACS numbers: 47.55.Mh

Recently, a great deal of interest has been focused on the investigation of transport phenomena in disordered systems [1]. In particular, fluid flow through porous media [2] has attracted much attention due to its importance in several technological processes (e.g., filtration, catalysis, chromatography, spread of hazardous wastes, petroleum exploration, and recovery, etc.). It is customary to model fluid flow in porous media by electrical transport, in particular, to relate the exponents of permeability and conductivity. In previous studies, computational simulations based on viscous fluid flow (Stoke's flow) [3] and lattice gas techniques [4] have been used to solve the problem of transversal flow through randomly generated porous media. Here we study fluid flow behavior by direct simulation of the Navier-Stokes equations in a percolation porous structure.

Our model for the pore connectivity is based on two-dimensional site percolation. Plaquettes (square obstacles) are randomly chosen and then removed from a 64×64 square lattice until, for the first time, a void space pathway (the "sample-spanning" cluster) can be detected connecting two opposite edges of the system [5]. At this point, the system achieves the percolation threshold. The sample-spanning cluster of sites connecting the network has a typical fractal geometry with fractal dimension $d_f \approx 1.896$ [1]. In percolation terminology, the "conducting backbone" is the connected subset of the sample-spanning cluster comprising bond elements which can carry current or flow. The remaining bonds attached to the sample-spanning cluster are called "dangling ends" and do not carry any electrical current.

We use nonslip boundary conditions at the entire solid-fluid interface. At the inlet and for each alive (fluid) cell of the lattice, we specify a constant inflow velocity in the normal direction to the boundary. At the exit, we assume the velocity gradient to be zero; further, we assume steady state flow in isothermal conditions, and that the Navier-Stokes and continuity equations for momentum and mass conservation hold [6]. The Reynolds number

$\text{Re} \equiv \rho d_p \overline{v}/\mu$, characterizes the relative contributions from convective and viscous mechanisms of momentum transfer in fluid flow, where ρ is the density, d_p is the particle diameter, μ is the kinematic viscosity, and $\overline{v}$ is the average fluid velocity.

For a given realization of the pore space with a specified void fraction ϵ and a fixed set of physical properties, the Navier-Stokes equations are solved for the velocity and pressure fields in the fluid phase of the pore space by discretization using the control volume finite-difference technique [7]. We implement grid elements with length equal to one-quarter of the solid cell size to generate satisfactory results when compared with numerical meshes of small resolution. The integral form of the governing equations is considered at each quadrilateral element of the numerical grid to render a set of coupled nonlinear algebraic equations which are pseudolinearized and sequentially solved [8]. Convergence is achieved when the overall sum of momentum and mass residuals falls below a specified value [9].

Initially, we study fluid flow under conditions of low Reynolds number ($\text{Re} = 0.0156$) to ensure that the contribution from inertial terms (convection) does not prevail over the viscous mechanism of momentum transfer. Figure 1(a) is a contour plot of the velocity magnitude for a typical realization at the percolation threshold $\epsilon = \epsilon_c$. In Fig. 2(a), we show a close-up section with a subset of the velocity vector field taken from the same realization of the pore space. The complex structure of the porous system at ϵ_c creates very tortuous pathways for fluid flow. A natural quantity to statistically characterize the fluid flow associated with each individual fluid cell in the numerical grid enclosing the physical pore space is the cell's kinetic energy $e \propto (v_x^2 + v_y^2)$, where v_x and v_y are the components of the velocity vector in the x and y directions.

Figure 3(a) shows the distribution $n(E)$ of the normalized kinetic energy $E \equiv e/e_{\max}$ for 4 network realizations, where $e_{\max}$ denotes the maximum kinetic energy
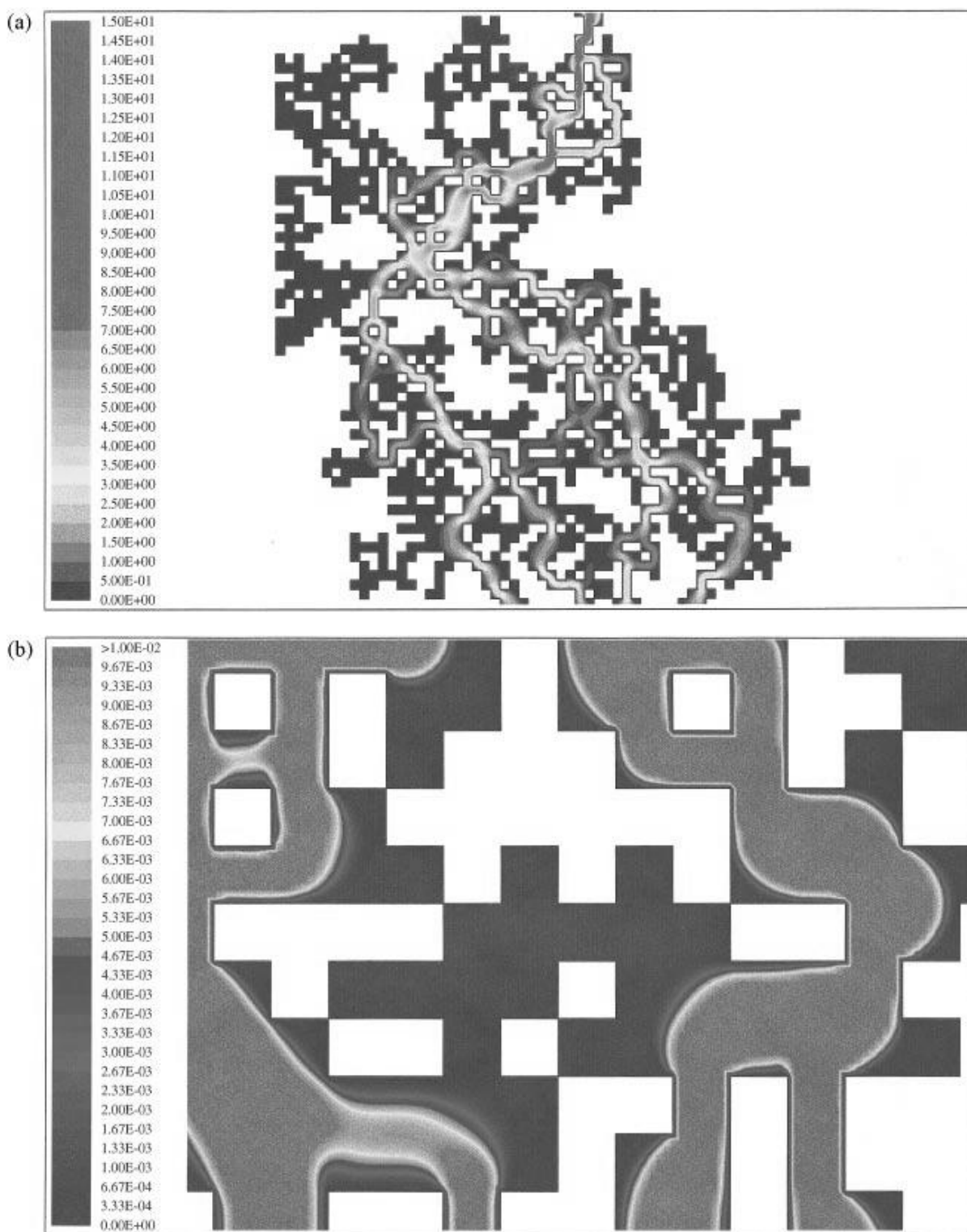
FIG. 1(color).   (a) Contour plot of the velocity magnitude for a typical realization of the infinite percolation cluster ($\epsilon = \epsilon_c$) on a 64×64 square lattice under low Re conditions (Re = 0.0156). (b) Contour plot of the local kinetic energy E for a typical realization under the same conditions as in part (a) ($\epsilon = \epsilon_c$, Re = 0.0156). The colors in the bar on the left correspond to different magnitudes of E. Values of $E > 10^{-2}$ are shown in red for better visualization of the fluid flow penetration into the "stagnant" zones.

observed for a given realization. We find that over roughly 5 orders of magnitude ($10^{-8} < E < 10^{-3}$), $n(E)$ follows

$$n(E) \propto E^{-\alpha}, \qquad (1)$$

with $\alpha = 0.90 \pm 0.03$. This power law behavior contrasts with the log-normal type of distribution found for the local current in the random resistor network model [10].
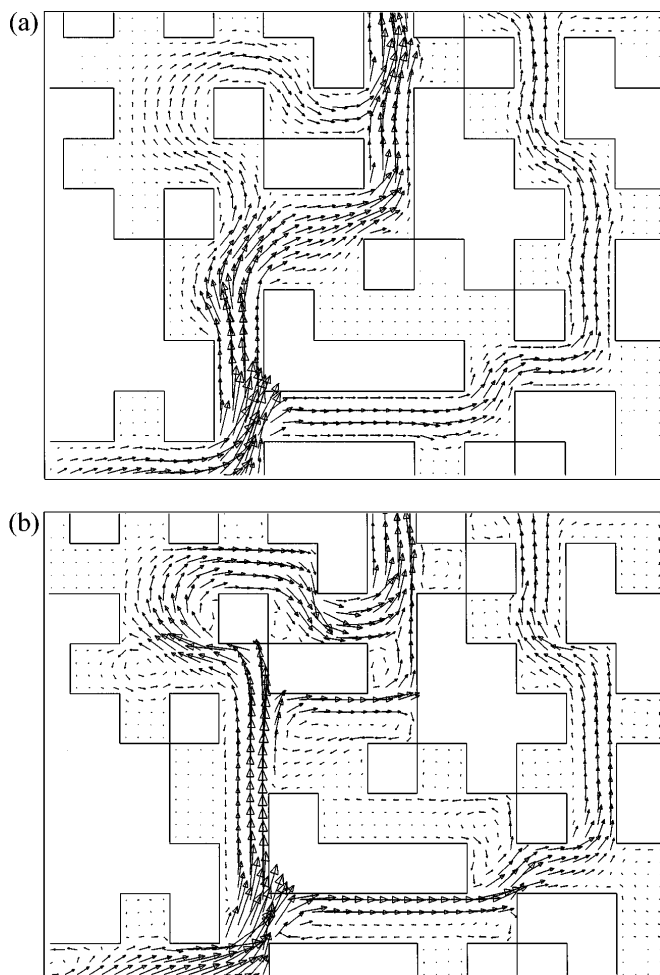
FIG. 2. (a) Subset of the velocity vector field taken from the same realization as in Fig. 1(a). Each vector represents the magnitude and direction of the local velocity. Fluid is pushed from bottom to top in the pore network. (b) Same subset as in part (a), but now for high Re conditions (Re = 156). The effect of inertia on the fluid flow is revealed by the presence of several vortices and zones of "flow separation." Note also that for flow at low Re [part (a)], the mainstream fluid pathway follows the shortest path through the backbone, while at high Re it does not. Instead, the mainstream fluid pathway is dictated by the local void space geometry.

The shape of the distribution $n(E)$ indicates that the local kinetic energy might be sensitive to the internal accessible perimeter of the disordered pore structure. This can be visualized from the contour plot shown in Fig. 1(b), where a limited subrange in the scaling region of variable E [see Fig. 3(a)] is arbitrarily chosen to be mapped inside the infinite cluster. Accordingly, this specific range of kinetic energy values corresponds to a thin fluid layer which moves relatively slowly compared to the mainstream flow, and hence approximately follows the internal perimeter of the infinite cluster. Indeed, by lowering this range of E values (down to the lower limit of $E \approx 10^{-8}$), we observe that fluid layers of even lower energies can penetrate into the pore space, and therefore experience more details of the landscape at the solid-fluid interface. Inside the "stagnant" zones of the infinite cluster, viscous
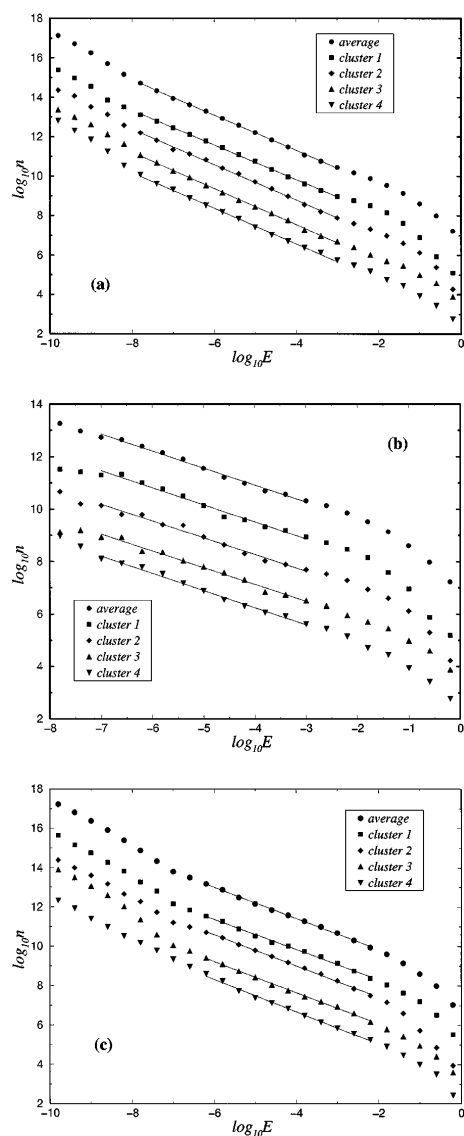

FIG. 3. (a) Double logarithmic plots for each of the four realizations of the distribution $n(E)$ of the local kinetic energy E under the same conditions as Fig. 1(a) ($\epsilon = \epsilon_c$, Re = 0.0156). The solid lines are least-squares fits to the data in the scaling region $10^{-8} < E < 10^{-3}$ ($\alpha = 0.87 \pm 0.02$, 0.89 ± 0.03, 0.92 ± 0.03, and 0.90 ± 0.02 for realizations 1, 2, 3, and 4, respectively). Also shown is the average over all four realizations, with slope $\alpha = 0.90 \pm 0.03$. Apart from the energy distribution of realization 1, all curves have been shifted for better visualization. (b) Same as part (a) except for the backbone. The average over all four realizations has slope $\alpha = 0.64 \pm 0.05$. Also, $\alpha = 0.65 \pm 0.05$, 0.63 ± 0.05, 0.63 ± 0.04, and 0.65 ± 0.04 for realizations 1, 2, 3, and 4, respectively. The solid lines are least-squares fits to the data in the scaling region $10^{-7} < E < 10^{-3}$. (c) Same as part (a) except for high Reynolds number (Re = 156). The average over all four realizations has slope $\alpha = 0.79 \pm 0.03$. For realizations 1, 2, 3, and 4, $\alpha = 0.76 \pm 0.03$, 0.79 ± 0.03, 0.78 ± 0.02, and 0.82 ± 0.03, respectively. The solid lines are least-squares fits to the data in the scaling region $10^{-6} < E < 10^{-2}$.

momentum is transmitted laterally across successive laminae of fluid and induces flow in the form of vortices that generate other vortices of smaller sizes and energies.

The upper cutoff value for the scaling region ($E \approx 10^{-3}$) determines the boundary line in the incipient infinite cluster that separates fluid cells located in the "stagnant" region of the pore space (low E values) from fluid cells in the main stream of fluid (high E values). These last elements move very fast through the inner part of the "backbone," and constitute a layer of moving fluid whose morphology is not directly affected by the internal perimeter of the percolation geometry. To test whether the power law behavior (1) arises from the transfer of momentum from the backbone through the stagnant zones in the percolation cluster, we calculated $n(E)$ separately for the backbone [Fig. 3(b)], and we find that $\alpha = 0.64 \pm 0.05$, a value quite different than for the full cluster.

We find that the exponent $\alpha = 0.90 \pm 0.03$ remains practically constant for Re $= 0.0156, 0.156$, and 1.56. We also studied the high Re case (Re $= 156$), using the parallel calculations as for low Re. We find that the data [see Fig. 3(c)] are consistent with the possibility that the exponent α is different for high Re ($\alpha = 0.79 \pm 0.03$). However, the magnitude of the difference, which is about 15%, is not so large. Further work is still needed to clarify this matter. At high values of Re, the nonlinear contribution from the convective terms in the Navier-Stokes equations becomes relevant. The inertial effect on the velocity field inside the infinite cluster is consistent with the presence of several vortices and zones of "flow separation" [Fig. 2(b)]. At low values of Re [see Fig. 2(a)], there is a tendency for the moving fluid at the local pore scale of the "flow backbone" to preserve the parabolic shape of the velocity profiles even if the fluid cells are confined to a very tortuous pathway. At high Re, on the other hand, the irregular geometry of the internal perimeter is very effective in producing sudden and dramatic changes in directions and magnitudes of mainstream velocity vectors, thus distorting their parabolic profile at the local level of the void space. These factors contribute to enhance the dissimilarities between the two scaling regimes.

Before concluding, we discuss the relation between our results in fluid flow through porous media and previous results for the flow of electricity in a percolation cluster, a system commonly used to model flow in porous media [10]. Our results indicate that the random resistor network model cannot be directly applied for fluid flow through porous materials, primarily due to viscous and inertial effects, which cause the log-normal distribution to cross over to the power law distribution found here. Moreover, the exponent α that we find is clearly sensitive to the transport of momentum into stagnant zones of the void space since it is 40% larger for the full cluster than for the backbone alone. In addition, we note that, while the void space in our description of the porous media is treated as a continuum, the traditional random resistor network represents a discrete electrical system. If considered as continuum, the dangling ends in the electrical problem could also modify the distribution of currents. Accordingly, an improved electrical percolation

analog for fluid flow at low Re conditions may apply if, e.g., each conducting cell in the random resistor network were replaced by many conducting elements.

In summary, we find by direct numerical solution of the Navier-Stokes equations in a percolation geometry that "stagnant" zones play an important role in the distribution $n(E)$ of local kinetic energy E, which follows a power law, $n(E) \propto E^{-\alpha}$, over roughly 5 orders of magnitude. The origin of the power law could be due to a multiplicative process involving random variables [11]. Our finding contrasts with the log-normal type of distribution found for the analogous electrical transport problem in the same structure [10], thereby providing a counterexample to the paradigm of electricity flow in random resistor networks and transport of mass and momentum in disordered porous media.

[1] M. Sahimi, *Applications of Percolation Theory* (Taylor & Francis, London, 1994).

[2] P. M. Adler, *Porous Media: Geometry and Transport* (Butterworth-Heinemann, Stoneham, MA, 1992).

[3] P. M. Adler, Transp. Porous Media **3**, 185 (1988); L. M. Schwartz, N. Martys, D. P. Bentz, E. J. Graboczi, and S. Torquato, Phys. Rev. E **48**, 4584 (1993); N. Martys, S. Torquato, and D. P. Bentz, Phys. Rev. E **50**, 403 (1994).

[4] D. H. Rothman, Geophysics **53**, 509 (1988); A. Canceliere, C. Chang, E. Foti, D. H. Rothman, and S. Succi, Phys. Fluids A **2**, 2085 (1990).

[5] We close the remaining two edges of the network with two additional columns of obstacles. This "insulating" condition reproduces more closely than periodic boundaries the experimental setup used to study fluid flow in real rocks.

[6] J. S. Andrade, Jr., D. A. Street, T. Shinohara, Y. Shibusa, and Y. Arai, Phys. Rev. E **51**, 5725 (1995).

[7] The FLUENT (trademark of FLUENT Incorporated) fluid dynamics analysis package was used in this study.

[8] S. V. Patankar, *Numerical Heat Transfer and Fluid Flow* (Hemisphere, Washington, DC, 1980).

[9] The criteria for convergence is defined here in terms of the "residuals" which provide a measure of the degree to which each conservation equation is satisfied throughout the flow field. Residuals are computed for each equation by summing the imbalance in the equation for all cells in the domain. The residuals for each flow variable (e.g., velocity, pressure, etc.) give a measure of the error magnitude in the solution at each iteration. In general, a solution can be considered well converged if the normalized residuals are on the order of 10^{-3}. In all simulations we performed, convergence is considered to be achieved only when the sum of the normalized residuals falls below 10^{-4}.

[10] L. de Arcangelis, S. Redner, and A. Coniglio, Phys. Rev. B **31**, 4725 (1985); **34**, 4656 (1986).

[11] B. J. West and M. F. Shlesinger, Int. J. Mod. Phys. B **3**, 795 (1989).